MOLECULAR CHARACTERIZATION OF *ASPERGILLUS PARASITICUS* AND *A. TERREUS* PRODUCING AND NON PRODUCING SILVER NANOPARTICLES USING DNA MARKERS

ABEER R. M. ABD-EL-AZIZ[a*], MONIRA R. AL-OTHMAN[a], MOHAMED A. MAHMOUD[b], SAMAH A. MONER[a]
[a]Botany and Microbiology Department, College of Science, King Saud University, Riyadh 1145, Saudi Arabia
[b]Plant Pathology Research Institute, Agricultural Research Center, Giza 12619, Egypt

Twelve aspergilli isolates were including two species *Aspergillus parasiticus* and *A. terreus*. *A. parasiticus* included six isolates, two isolates producing sliver nanoparticles (AgNPs) and four isolates non producing AgNPs. *A. terreus* enclosed six isolates with a similar description. Random amplified polymorphic DNA (RAPD) and Inter simple sequence repeats (ISSR) DNA markers were used, with the aim of genetically characterizing isolates of *A. parasiticus* and *A. terreus* to discriminate between producing and non producing AgNPs isolates**.** RAPD and ISSR analysis revealed a high level of genetic diversity in the *Aspergillus parasiticus* and *A. terreus* population, useful for genetic characterization**.** *A. parasiticus* and *A. terreus* isolates (producing and non producing AgNPs) shown in RAPD and ISSR dendrogram with a random distribution. There was no clear-cut relationship between the RAPD and ISSR markers and AgNPs production. RAPD and ISSR markers were not suitable to discriminate between producing and non producing AgNPs isolates**.**

1. Introduction

In recent times, many methods have been designed to synthesize nanoparticles such as physical method, chemical method and biological methods [1]. Synthesis of nanoparticles has been demonstrated by the use of biological agents like bacteria, fungi, yeast and plants [2]. The fungal system in recent times has emerged as "Bionanofactories" synthesizing nanoparticles of gold, CdS, platinum, silver, and etc [3], [4], [5], [6]). The biological route for the synthesis of nanoparticles implying the use of fungi is advantageous over the traditional methods, as biological synthesis is cost-efficient, environment-friendly and gaining control over the size and shape of nanoparticles and simple method ([7], [8]). The fungal system shows the capability of both intracellular (*Verticillium luteoalbum* and *Aspergillus flavus*) [3], [9]) and extracellular (*Fusarium oxysporum*, *Aspergillus niger* and *Aspergillus terreus* KC462061) [10], [11], [6]) synthesis of nanoparticles.

As PCR technology finds increased use in genetic analysis, novel variations of this technique are emerging which promise precision, economy and speed. Molecular genetic analysis using DNA markers would provide valuable tools for detection genetic relationship among a unique population like *Aspergilli* [12].

The random amplified polymorphic DNA (RAPD) technique has been used to characterize and detect genetic variability between isolates of *A. flavus* and related species [13], [14], [15]).

---

*Corresponding author: aabdelaziz@ksu.edu.sa

The inter-simple sequence repeats (ISSR) technique has been employed to investigate the diversity and population structure of *A. flavus* [16], [17], [18]). The aim of the present study was to genetic characterization of *Aspergillus parasiticus* and *A. terreus* isolates producing and non producing silver nanoparticles (AgNPs) using RAPD and ISSR markers.

2. Materials and methods

A. parasiticus-specific PCR assay

Specific PCR assays were carried out using primers PAR1 and PAR2 for *A. parasiticus* [19]. Sequences of the primers used shown in Table 1. The PCR amplification protocol used for *A. parasiticus* was amplification reactions were carried out in volumes of 25 ml containing 2 ml (10–80 ng) of template DNA, 1 ml of each primer (20 mM), 2.5 ml of 10X PCR buffer, 1 ml of MgCl2 (50 mM), 0.2 ml of dNTPs (100mM) and 0.2 ml of Taq DNA polymerase (5 U/ml) supplied by the manufacturer (BioLabs, UK). Amplification parameters for primer sets used are presented in Table 2

Table 1. Sequences of the nucleotide primers used in this study.

Primer	Sequence	Target	References
Aspergilli-specific PCR assay			
PAR1	5-GTCATGGCCGCCGGGGGCGTC-3	*A. parasiticus*	[19]
PAR2	5-CCTGGAAAAAATGGTTGTTTTGCG-3		
ATE1	5′-CTA TTG TAC CTT GTT GCT GGCG-3′	*A. terreus*	[20]
ATE2	5′-AGT TGC AAA TAA ATG CGT CGG CGG-3′		
RAPD-PCR			
GL-Decamer B-09	5` TGGGGGACTC 3	*A. parasiticus*	[15]
GL-Decamer B-10	5` CTGCTGGGAC 3		
OPB3	GATCCCCCTG		[21]
PG01	5'-CAG GTG TTG C-3'	*A. terreus*	[22]
PG02	5'-CTG GAC AGA C-3'		
P4	5'-GATAGATAGATAGAT-3'		[23]
ISSR-PCR			
(GTG)5	5'-GTG GTG GTG GTG GTG-3'	*A. parasiticus*	[13]
(GACA)4	5'-GAC AGA CAG ACA GAC A-3		
(AGAG)4G	5'-AGA GAG AGA GAG AGA GG-3'		[24]
ISSR 7	5′-AGA GCG AGG AGG AGG AGG AGG-3′	*A. terreus*	[25]
ISSR 9	5′-AGA GCG CTC CTC CTC CTC CTC-3′		
ISSR 13	5′-AGA GCG CGC ACG CAC GCA CGC A-3′		

Table 2. Amplification parameters for all primer sets used.

Primer name	PCR conditions
PAR1 and PAR2	1 cycle at 95°C 5 min, 26 cycles (95°C 30 s, 69.3°C 30 s , 72°C 30 s), 72°C 5 min.
ATE1 and ATE2	1 cycle at 95°C for 5 min, 35 cycles (94°C 1 min, 59°C 1 min., 72°C 1.5 min), 72°C 5 min.
GL-Decamer B-09 and B-10	1 cycle at 94°C for 5 min, 34 cycles (94°C 40 s, 3°C for 30 s,72°C 90 s), 72 °C 10 min.
OPB3	1 cycle at 94°C 4 min, 40 cycles (94°C 30 s., 35°C 1 min, 72°C 2 min), 1 cycle at 72°C 5 min, 1 cycle at 40°C 10 min.
PG01 and PG02	1 cycle at 92°C 5 min, 34 cycles (94°C 40 s, 36°C 30 s, 72°C 1.5 min) 72°C 5 min.
P4	1 cycle at 94°C 5 min, 30°C 30 min, 72°C 1 min, 35 cycles (94°C 1 min, 36°C 1 min, 72°C 1.5 min), 5 cycles (94°C 1 min, 36°C 1 min, 72°C 5 min), 72°C 5 min.
$(GTG)_5$, $(GACA)_4$ and $(AGAG)_4G$	1cycle at 92°C for 5 min followed by 40 cycles (92°C 1 min, 39°C 1.5 min, 72°C 2 min) 72°C for 5 min.
ISSR 7, 9 and 13	95°C 5 min, 36 cycles (93°C 50 s, 50°C 45 s, 72°C 2 min), 72°C 5 min.

A. terreus-specific PCR assay

Specific PCR assays were carried out using primers ATE1 and ATE2 for *A. terreus* [20]. Sequences of the primers used shown in Table 1. Amplification reactions for *A. terreus* were carried out in volumes of 20 μL containing 2 μL (10 pg- 10 ng) of template DNA, 1.2 μL of each primer (20 pmole), 2.5 μL of 10x PCR buffer (BioLabs), 1 μL of $MgCl_2$ (50 mM), 2 μL of dNTPs mixture (100 mM) and 0.2 μL of Taq DNA polymerase (5 U/μL) supplied by the manufacturer (BioLabs) and water adjusted to a final volume of 20 μL. Amplification parameters for all primer sets used are presented in Table 2.

RAPD-PCR for *A. parasiticus*

The three primers selected with high reproducibility and clear banding profiles were the RAPD primers GL DecamerB-09, GL DecamerB-10 [15] and OPB3 [21]. Sequences of the primers used shown in Table 1. The PCR mixtures were made to a final volume of 25 μL, containing reaction buffer (20 mM Tris-HCl, pH 8.4, 50 mM KCl) (BioLabs), 3.4 mM $MgCl_2$, 0.25 mM dNTP, 0.4 mM of each primer, 2 U Taq DNA polymerase (BioLabs), and 25 ng genomic DNA. Amplification parameters for primer sets used are presented in Table 2.

RAPD-PCR for *A. terreus*

The three RAPD primers PG01, PG01 [22] and P4 [23] were used for amplifications. Sequences of the primers used shown in Table 1. The PCR mixtures were made as pervious method. Amplification parameters for primer sets used are presented in Table 2.

ISSR-PCR for *A. parasiticus*

PCR amplification of ISSR was performed with $(GTG)_5$, $(GACA)_4$ [13], and $(AGAG)_4G$ [24] primers. Sequences of the primers used shown in Table 1. The reaction mixtures were made to a final volume of 25 μL, containing reaction buffer (20 mM Tris-HCl, pH 8.4, 50 mM KCl), 1.5 mM MgCl2, 0.25 mM dNTP, 0.25 mM primer, 2.0 U Taq DNA polymerase (BioLabs), and 25 ng genomic DNA. Amplification parameters for primer sets used are presented in Table 2.

ISSR-PCR for *A. terreus*

The three ISSR primers ISSR 7, ISSR 9 and ISSR [25] were used for amplifications. Sequences of the primers used shown in Table 1. The PCR mixtures were made as pervious method. Amplification parameters for primer sets used are presented in Table 2.

PCR reactions were performed in a Techne thermal cycler (TC-512-Techne) (Staffordshire, UK). PCR products were separated by 1.5% agarose gel electrophoresis in 1X TAE buffer (Tris-acetate EDTA, pH 8.0) at 100 V for 50 min, using a 100-bp ladder DNA marker (Intron, Korea). DNA was visualized by UV light after staining with ethidium bromide.

3. Results

A. parasiticus-specific PCR assay

A single fragment of about 430 bp was only amplified when genomic DNA from *A. parasiticus* isolates was used (Fig. 1), but not from *A. terreus*. No product was observed with genomic DNA from *A. terreus* isolates.

Fig. 1. PCR amplification profile of genomic DNA of two isolates of Aspergillus species group primers PAR1 and PAR2. Lanes 1 to 6 (A. parasiticus) and lanes 7-12 (A. terreus) A. terreus. Arrows point to a 430-bp band of a 100-bp DNA ladder marker (M).

A. terreus-specific PCR assay

A unique band of about 450 bp was only amplified when genomic DNA from *A. terreus* isolates was used (Fig. 2), but not from *A. parasiticus*. No product was observed with genomic DNA from *A. parasiticus* isolates.

Fig. 2. PCR amplification profile of genomic DNA of two isolates of Aspergillus species group primers PAR1 and PAR2. Lanes 1 to 6 (A. parasiticus) and lanes 7-12 (A. terreus) A. terreus. Arrows point to a 450-bp band of a 100-bp DNA ladder marker (M).

Phenetic analysis of the 6 *A. parasiticus* isolates based on 3 RAPD primers Primer GL-Decamer B-09

The dendrogram generated using the similarity matrix produced from the banding patterns obtained with GL-Decamer B-09 exhibited the genetic similarity (GS) between the tested isolates ranged from 77.4% to 93.1% (Fig. 3A). The dendrogram divided into two main clusters, with 63.82% GS. The dendrogram divided into two main clusters, with 77.4% GS. The first main cluster contained three isolates KSU-07, KSU-17 (producing AgNPs) and KSU-04 (non producing AgNPs), which showed 85.6% GS. The second main cluster contained three isolates KSU-24, KSU-11, and KSU-15 (non producing AgNPs), which showed 81.6% GS.

Primer GL-Decamer B-10

A cluster analysis was performed based on the similarity matrix with GL-Decamer B-10, showed the GS ranged from 70.4% to 93.7% GS (Fig. 3B). A cluster analysis split into two main clusters, with 70.4% GS. The first main cluster contained four isolates, three KSU-04, KSU-11 and KSU-24 (non producing AgNPs) and KSU-12 (producing AgNPs), which showed 83.6% GS.

The second main cluster involved two isolates, KSU-07 (producing AgNPs) and KSU-15 (non producing AgNPs), which displayed 81.4% GS.

Primer OPB3

UPGMA dendrogram based on the similarity matrix with OPB3 displayed the GSs for isolates ranged from 75.3% to 95.6% between the isolates were tested (Fig. 3C). UPGMA dendrogram split into two main clusters, with 75.3% GS. The first main cluster contained three isolates, two KSU-11, KSU-24 (non producing AgNPs) and KSU-07 (producing AgNPs), which showed 87.2% GS. The second main cluster involved three isolates, two KSU-07, KSU-15 (non producing AgNPs) and KSU-12 (producing AgNPs), which displayed 84.1% GS.
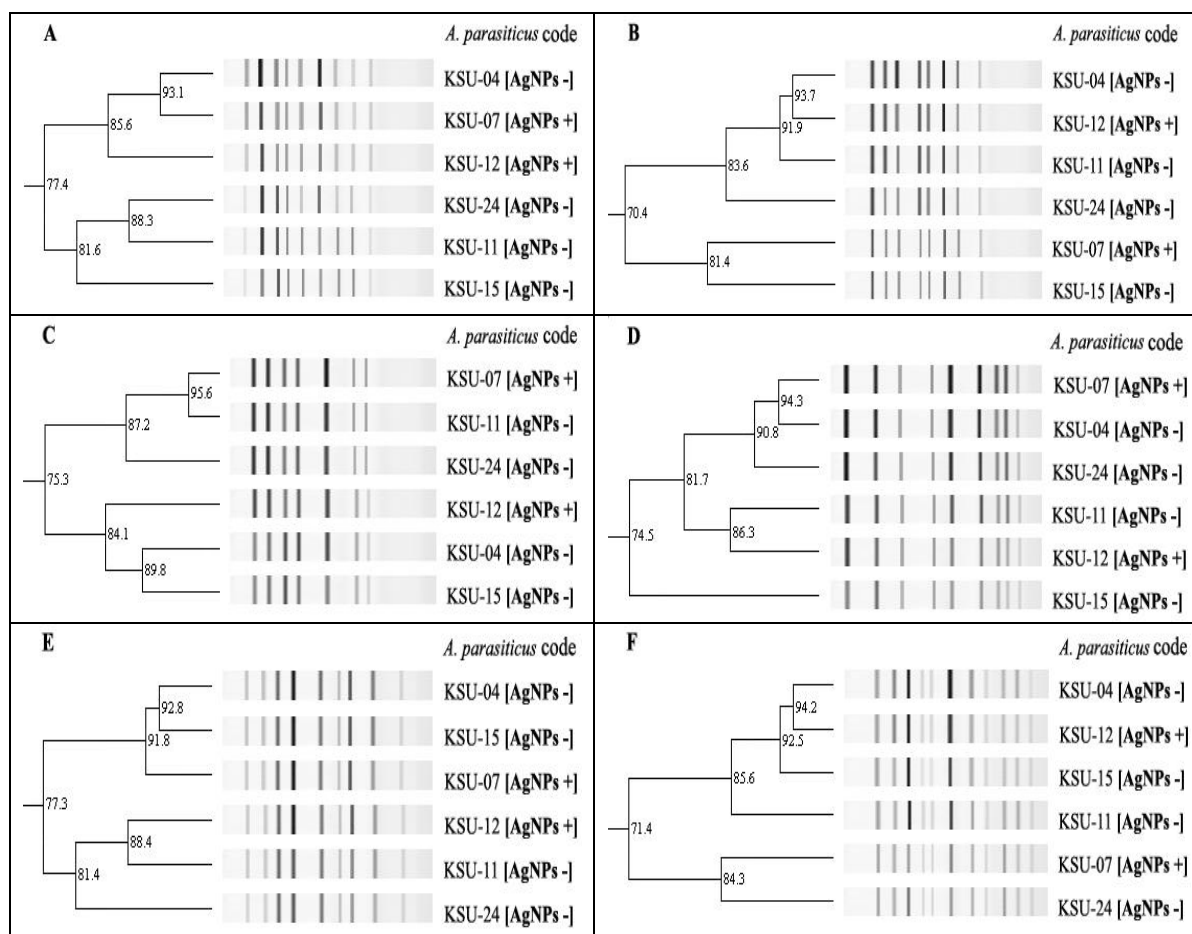
Fig. 3. Dendrogram obtained by UPGMA method derived from PCR amplification banding of RAPD and ISSR primers with A. parasiticus. RAPD primers, (A) GL-Decamer B-09, (B) GL-Decamer B-10 and (C) OPB3. ISSR primers, (D) primer $(GTG)_5$, (E) primer $(GACA)_4$ and (F) primer $(AGAG)_4G$.

Phenetic analysis of the 6 *A. parasiticus* isolates based on 3 ISSR primers
Primer $(GTG)_5$

The dendrogram generated using the similarity matrix with $(GTG)_5$ exhibited the GSs between the tested isolates ranged from 74.5% to 94.3% (Fig. 3D). The dendrogram split into two main clusters, with 74.5% GS. First main cluster included two groups at 81.7% GS. The first group included three isolates, two KSU-04, KSU-24 (non producing AgNPs) and KSU-07 (producing AgNPs), which showed 90.8% GS. The second group involved two isolates, KSU-11 (non producing AgNPs) and KSU-12 (producing AgNPs), which displayed 86.3% GS. The second main cluster has only one isolate, KSU-15 (non producing AgNPs).

Primer $(GACA)_4$

A cluster analysis was performed based on the similarity matrix with primer $(GACA)_4$, was appeared the GSs between the tested isolates ranged from 77.3% to 92.8% (Fig. 3E). A cluster analysis split into two main clusters with 77.3% GS. The first main cluster contain three isolates, two isolates KSU-04, KSU-14 (non producing AgNPs) and one KSU-07 (producing AgNPs), which showed 91.7% GS. The second main cluster consisted of three isolates, two isolates KSU-11, KSU-24 (non producing AgNPs) and one KSU-12 (producing AgNPs), which displayed 81.4% GS.

Primer $(AGAG)_4G$

The dendrogram generated using the similarity matrix obtained with $(AGAG)_4G$ GSs between the tested isolates ranged from 71.4% to 94.2% (Fig. 3F). The dendrogram divided into

two main clusters, with 71.4% GS. The dendrogram divided into two main clusters, with 77.4% GS. The first main cluster contained four isolates, three KSU-04, KSU-15, KSU-11 (non producing AgNPs) and KSU-12 (producing AgNPs), which displayed 85.6% GS. The second main cluster contained two isolates, KSU-07 (producing AgNPs), KSU-24 (non producing AgNPs) which showed 84.3% GS.

Phenetic analysis of the 6 *A. terreus* isolates based on 3 RAPD primers
Primer PG1
A cluster analysis was performed based on the similarity matrix with PG1, was appeared the GSs between the tested isolates ranged from 67.3% to 94.1 % (Fig. 4A). A cluster analysis divided into two main clusters with 67.3% GS. The first main cluster contain four isolates, two isolates KSU-18, KSU-05 (non producing sliver nanoparticles) and two isolates KC462061, KSU-34 (producing sliver nanoparticles), which showed 81.8% GS. The second main cluster consisted of two isolates non producing sliver nanoparticles (KSU-09 and KSU-33), which displayed 80.2% GS.
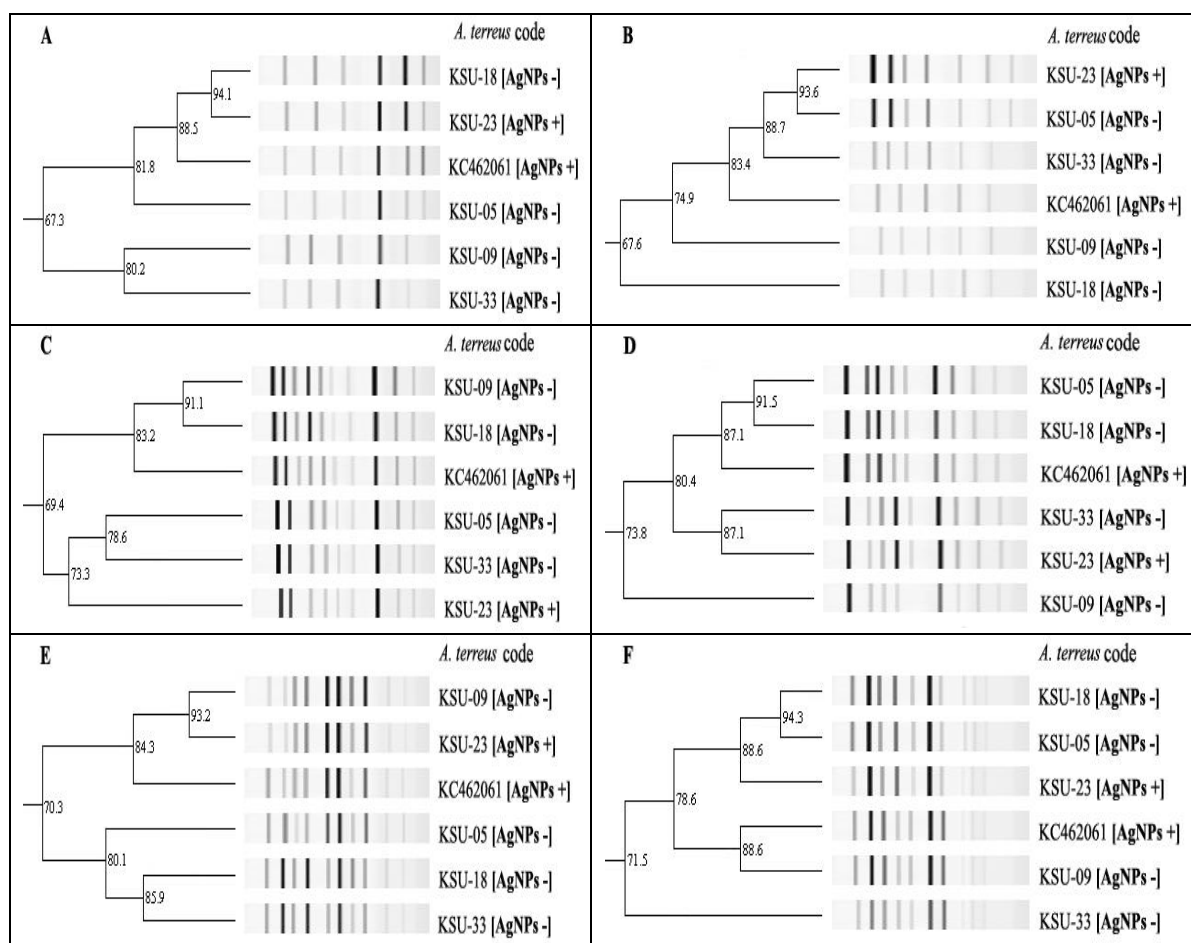

Fig. 4: Dendrogram obtained by UPGMA method derived from PCR amplification banding of RAPD and ISSR primers with A. terreus. RAPD primers, (A) PG1, (B) PG2 and (C) P4. ISSR primers, (D) ISSR7, (E) ISSR 9 and (F) ISSR 13.

Primer PG2
The dendrogram generated using the similarity matrix with PG2 was appearing overlapping between the tested isolates (Fig 4B). The GSs between the tested isolates ranged from 67.6% to 93.6% GS. Only clear one subcluster included two isolates KSU-23 (producing sliver nanoparticles) and KSU-05 (producing sliver nanoparticles), which displayed 93.6% GS.

Primer P4

UPGMA dendrogram based on the similarity matrix with P4 displayed ranged from 69.4% to 91.1% GS between the isolates (Fig. 4C). UPGMA dendrogram divided into two main clusters with 69.4% GS. The first main cluster contain three isolates, two isolates KSU-09, KSU-18 (non producing sliver nanoparticles) and one KC462061 (producing sliver nanoparticles), which showed 83.2% GS. The second main cluster consisted of three isolates, two isolates KSU-05 and KSU-33 (non producing sliver nanoparticles) and one KSU-23 (producing sliver nanoparticles), which displayed 73.3% GS.

Phenetic analysis of the 6 *A. terreus* isolates based on 3 ISSR primers
Primer ISSR 7

A cluster analysis was performed based on the similarity matrix with ISSR 7, was appeared the GSs ranged between the tested isolates from 73.8% to 91.5 % (Fig. 4D). A cluster analysis divided into two main clusters with 73.8% GS. The first main cluster included three isolates, two isolates KSU-05, KSU-18 (non producing sliver nanoparticles) and one KC462061 (producing sliver nanoparticles), which showed 87.1% GS. The second main cluster consisted of two isolates KSU-33 (non producing sliver nanoparticles) and KSU-23 (producing sliver nanoparticles) and one KSU-23 (producing sliver nanoparticles), which displayed 87.1% GS. The second main cluster consisted of only one isolate, KSU-09 (non producing sliver nanoparticles).

Primer ISSR 9

The dendrogram generated using the similarity matrix with ISSR 9 exhibited the GSs between the tested isolates ranged from 70.3% to 93.3% (Fig. 3E). The dendrogram divided into two main clusters with 70.3% GS. The first main cluster included three isolates, two isolates producing sliver nanoparticles (KSU-23, KC462061) and one non producing sliver nanoparticles (KSU-09), which showed 84.3% GS. The second main cluster consisted of three isolates KSU-05, KSU-18 and KSU-33 (non producing sliver nanoparticles), which displayed 80.1% GS.

Primer ISSR 13

UPGMA dendrogram based on the similarity matrix with ISSR 13 displayed the GS ranged from 71.5% to 94.3% GS between the isolates were tested (Fig. 3F). UPGMA dendrogram divided into two main clusters with 71.5% GS. The first main cluster included two groups with 81.5% GS. The first group contained three isolates, two isolates KSU-15, KSU-09 (non producing sliver nanoparticles) and KSU-12 (producing sliver nanoparticles), which showed 88.6% GS. The second group included two isolates KSU-06 (non producing sliver nanoparticles) and KSU-29 (producing sliver nanoparticles) which displayed 85.2% GS. The second main cluster consisted of only one isolate, KSU-27 (non producing sliver nanoparticles).

Aspergilli isolates producing and non producing sliver nanoparticles established in a random distribution with RAPD and ISSR primers which indicating no correlation was detected between the DNA banding patterns obtained and AgNPs-producing ability.

5. Discussion

We have carried out a specific PCR protocol for the identification of *A. parasiticus,* the protocol described is a useful tool for accurate discrimination *A. parasiticus* from the other related *Aspergillus* species. PCR-based methods that target DNA are considered a good alternative for rapid diagnosis due to their high specificity and sensitivity, and have been used for the identification of *A. parasiticus* [19], [26], [27]. A specific and highly sensitive PCR protocol was developed to detect *A. parasiticus* using primers designed on the multicopy internal transcribed region of the rDNA unit (ITS1-5.8S-ITS2 rDNA). PCR protocol based on multicopy sequences (ITS) specific to *A. parasiticus* which allows distinction from other *Aspergilli*, in particular from *A. flavus* [19]. The ITS 1–5.8S–ITS 2 region of *A. terreus* was chosen for the design of the ATE1–ATE2 specific primer set, due to availability of nucleotide data regarding *A. terreus*. Furthermore, both ITS 1 and 2 regions are necessary for species level identification [28], [20].

RAPD fingerprints were used to analysis genetic relationships among *A. niger*, A. *flavus* and A. *parasiticus*. RAPD markers used to gain rapid and precise information about genetic similarities and dissimilarities of different Aspergillus species. RAPD fingerprints of *A. niger*, *A. flavus* and *A. parasiticus* revealed polymorphism in 37, 59, 51% of the analyzed *Aspergillus* sp. [21]. RAPD study is useful in estimating distances between and within same *Aspergillus* species (*A. niger*, *A. nidulans*, *A. parasiticus*, *A. japonicas*, *A. fumigates*, *A. oryzae* and *A. flavus*) and might help future programs of management and conservation. Genetic differences between species of the same genus maintain characterization and genetic diversity within this population [15]. Microsatellite analysis of 84 Vietnamese *A. flavus* strains (isolated from corn and peanut) revealed high genetic diversity [16]. ISSR analysis can be useful in population genetic analyses, epidemiological surveys and ecological studies of *A. flavus*. Additionally the $(GTG)_5$ primer can be applied to generate unique products from different *Aspergillus* species that can then be converted to sequences, and the characterized amplified regions can aid in taxonomic identification [13]. Phylogeny tree based on RAPD-PCR profile was sufficient in genotyping of *A. terreus* isolates collected from arid regions of Iraq and showed variable degrees of similarity among 19 isolates of *A. terreus* and divided them into many genotypes [29]. Genomic profile of five *A. terreus* isolates isolated from the dried grapes, through RAPD analysis calefaction different discriminations among the isolates also, there was a homology of genotype between the isolates. Low similarity was detected for isolates indicating great genomic diversity of *A. terreus* [22]. Molecular typing for clinical isolates of *A. terreus*, based on RAPD-PCR patterns. These variations in the patterns may contribute in clarification and explanation of the sources of phenotypic variations especially in colonies colors and pigments of *A. terreus* [23]. A total of 117 clinical *A. terreus* isolates originating from France or Belgium (28 isolates), Italy (46 isolates), and the Eastern (22 isolates) and Western (21 isolates) United States. Inter-Simple Sequence Repeat (ISSR) PCR was used to assess the use of this fingerprinting method for discriminatory genotyping of *A. terreus*. *A. terreus* isolates collections were genotyped as highly discriminatory genome-wide DNA fingerprinting [25].

Aspergilli isolates producing and non producing sliver nanoparticles established in a random distribution with RAPD and ISSR primers which indicating no correlation was detected between the DNA banding patterns obtained and AgNPs-producing ability. As RAPD and ISSR techniques amplified fragments of the fungal genome, the fragment that contained CRM (Common Metal Responsive) genes may not have been amplified using these techniques with the used primers because these genes need specific primers.

Genome, transcriptome, deletome, proteome, metabolome and interactome analyses have been performed and are in progress to learn how different fungi respond to versatile toxic metal/metalloid exposures. To become familiar with the elements and the regulation of the metal/metalloid stress response networks may provide us with suitable tools to augment the metal/metalloid tolerance of selected fungi [30].

Identify the group of CRM (Common Metal Responsive) genes, which may provide us with the possibility to construct fungal strains with a general metal/metalloid tolerance! Over expressions of genes encoding e.g. polyamine and iron transporters, proteins maintaining ion homeostasis and iron transport as well as elements of the antioxidant defense system, or elimination of genes encoding e.g. protein kinase subunits and transition metal and carbohydrate transporters [31]. The extracellular synthesis of silver nanoparticles by silver-tolerant yeast strain MKY3. The exact mechanism leading to the reduction of silver ions is not yet understood and the authors postulated that biochemical reducing agents are secreted by the yeast cells in response to silver stress [32]. It could not find the exact mechanisms of formation of gold and silver nanoparticles by *Verticillium* sp. Since the nanoparticles are formed on the surface of the mycelia and not in the solution, they believed that the first step involves trapping of the Ag+ ions on the surface of the fungal cells, possibly via electrostatic interaction between gold ions and negatively charged carboxylate groups in enzymes present in the cell wall of the mycelia. Thereafter, the silver ions are reduced by enzymes present in the cell wall leading to the formation of silver nuclei, which subsequently grow by further reduction of Ag ions and accumulation on these nuclei [33]. The aqueous extract of the fungal biomass can reduce gold and silver ions to the corresponding nanoparticles. Apart from individual metal nanoparticles, the formation of highly

stable Au–Ag alloy by *F. oxysporum* was observed. Variation in the amount of biomass used in the experiment reveals that the secreted cofactor NADH plays an important role in determining the composition of Au–Ag alloy nanoparticles.

The authors suggested that the reduction of Au+3 and Ag+1 ions occurs due to reductases released by the fungus into the solution [34]. It was later demonstrated that a nitrate-dependent reductase and shuttle quinine from several *F. oxysporum* strains were involved in the extracellular synthesis of silver nanoparticles. However, it was not true with all strains of *Fusarium*. For example, *Fusarium moniliforme* produced reductase enzyme but could not form silver nanoparticles during the incubation with silver ions. Thus, the probable mechanism of silver reduction includes the conjugated oxidation–reduction reactions of electron carriers in which NADP-dependent nitrate reductase takes part [35]. More recently, [36] and [37] demonstrated extracellular biosynthesis of silver nanoparticles by Fusarium semitectum and *Fusarium solani* (USM-3799). The results obtained from these studies suggested that the protein might have played an important role in the reduction of Ag+ and in the stabilization of silver nanoparticles through coating of protein moiety on the silver nanoparticles.

It seems that microbes produce nanoparticles as a consequence of the detoxification pathway. But the mechanism of bioreduction of metal ions is still an open question. I believe that many more possible mechanisms are involved in this process.

6. Conclusion

Aspergilli isolates producing and non producing sliver nanoparticles established in a random distribution with RAPD and ISSR primers which indicating no correlation was detected between the DNA banding patterns obtained and AgNPs-producing ability. As RAPD and ISSR techniques amplified fragments of the fungal genome, the fragment that contained CRM (Common Metal Responsive) genes may not have been amplified using these techniques with the used primers because these genes maybe need specific primers.

Acknowledgments

References

[1] J. M. Kohler, U. Hubner, H. Romanus, J. Wagner, Journal of Nanomaterial **1155**, 98134 (2007)

[2] M. Rai, A. Yadav, A. Gade, Critical Reviews in Biotechnology **28,** (4) 277 (2008).

[3] M. Gericke, A. Pinches, Gold Bulletin. **39**(1), 22 (2006)

[4] A. S. Kumar, A. A. Ansary, A. Ahmad, M. I. Khan, Journal of Biomedical Nanotechnology **3**, 190 (2007).

[5] Y. Govender, T. Riddin, M. Gericke, C. G. Whiteley, Biotechnology Letters **31**(1), 95 (2009).

[6] M. R. Al-Othman, A. R. M.Abd El-Aziz, M. A. Mahmoud, S. A. Eifan, M. S. El-Shikh, M. Majrashi, Digest Journal of Nanomaterials and Biostructures **9**(1) 151 (2014).

[7] T. L. Riddin, M. Gericke, C. G. Whiteley, Nanotechnology **17**, 3482 (2006).

[8] P. Mukherjee, M. Roy, B. P. Mandal, G. K. Dey, P. K. Mukherjee, J. Ghatak, A. K. Tyagi, S. P. Kale, Nanotechnology **19**, 103 (2008).

[9] N. Vigneshwaran, M. Ashtaputre, R. P. Nachane, K. M. Paralikar, H. Balasubramanya, Material Letters. **61**(6) 1413 (2007).

[10] A. Mohammadian, S. A. Shaojaosadati, M. H. Rezee, Scientia Iranica. **14**(4), 323 (2007).

[11] A.P. Ingle, A.K. Gade, S. Pierrat, C. Sonnichsen, M.K. Rai, Curr Nanosci **4**, 141 (2008)

[12] F, Bardakci, Turk. J. Biol. **25**, 185 (2001).

[13] P. P. Batista J. F. Santos, N. T. Oliveira, A. P. Pires, C. M. S. Motta, E. A. Luna-Alves Lima, Genet. Mol. Res. **7**, 706 (2008).

[14] P. Gehlot, D. K. Purohit, S. K. Singh, Indian J. Biotechnol. **10**, 207 (2011).

[15] S. Irshad, R. Nawab, Journal of Microbiology Research **2**, 47 (2012).

[16] N. Tran-Dinh, I. Kennedy, T. Bui D. Carter (2009). Mycopathologia **168**, 257 (2009)

[17] I. Hadrich, F. Makni, A. Ayadi, S. Ranque, J. Clin. Microbiol. **48**, 2396 (2010).

[18] X. Wang, P. A. Wadl, A. Wood-Jones, G. Windham, Mycopathologia **174**, 371 (2012).

[19] N. Sardiñas, C. Vázquez, J. Gil-Serna M. T. González-Jaen, B. Patiño, Food Addit Contam. **27**(6), 853 (2010).

[20] M. Logotheti, A. Kotsovili-Tseleni, G. Arsenis, N. I. Legakis, Journal of Microbiological Methods **76**, 209 (2009).

[21] N. Aiat, Journal of Applied Sciences Research **2**(10), 709 (2006).

[22] B. Narasimhan, M. Asokan, Advances in Bioscience and Biotechnology **1**, 345 (2010).

[23] C. Lass-Flörl K. Grif P. Dimitrios, Journal of clinical microbiology, **45**, 2686 (2006).

[24] A.D.,Hatti S.D. Taware, A.S. Taware, P.P. Pangrikar, A.M. Chavan, D.S. Mukadam, Int. J. Curr. Res. **5**, 61 (2010).

[25] O.S. Neal, A.O. Richardson, S. F. Hurst, A. M. Tortorano, M. A. Viviani, D. A. Stevens, S. A. Balajee, BMC Microbiology **11**, 203 (2011).

[26] D. Somashekar, E. R. Rati, A. Chandrashekar, Int J Food Microbiol **93**, 101 (2004).

[27] A. Gonzalez-Salgado, M. T. Gonzalez-Jaen, C. Vazquez, B. Patino, Food Addit Contam **25**, 758 (2008).

[28] T. Henry, P. C., Iwen, S. H. Hinrichs, J. Clin. Microbiol. **38**(4), 1510 (2000).

[29] Z. K., Imra, A. A. Al-Rubaay, International Journal of Advanced Research **2**(3), 1041 (2014).

[30] I. Pócsi Toxic Metal/Metalloid Tolerance in Fungi-A Biotechnology-Oriented Approach, Cellular Effects of Heavy Metals, Gaspar Banfalvi, pp 31-58, (2011).

[31] Y. H. Jin, P. E. Dunlap, S. J. McBride, H. Al-Refai, P. R. Bushel, J. H. Freedman, PLoS Genet **4**(4), (2008)

[32] M. Kowshik, S. Ashtaputre, S. Kharrazi, W. Vogel, J. Urban, S. K. Kulkarni K. M. Paknikar, Nanotechnology **14**, 95 (2003).

[33] P. Mukerjee, A. Ahmad, D. Mandal, S. Senapati, S. R. Sainkar, M. I. Khan, R. Parischa, P. V. Ajayakumar, M. Alam, R. Kumar, M. Sastry, Nano Lett **1**, 515 (2001).

[34] S. Senapati, A. Ahmad, M. I. Khan, M. Sastry, R. Kumar, Small **1**, 517 (2005).

[35] N. Duran, P. D. Marcato, O. L. Alves, G. DeSouza, E. Esposito, J Nanobiotechnol **3**, 1 (2005).

[36] S. Basavaraja, S. D. Balaji, A. Lagashetty, A. H. Rajasab, A. Venkataraman, Mater Res Bull **43**(5), 1164 (2008).

[37] A. Ingle, M. K. Rai, A. Gade, M. Bawaskar, Journal of Nanoparticle Research. **11**(8), 2079 (2009).